

Focal Adhesion Dynamics Are Altered in Schizophrenia

Yongjun Fan, Greger Abrahamsen, Richard Mills, Claudia C. Calderón, Jing Yang Tee, Lisette Leyton, Wayne Murrell, Justin Cooper-White, John J. McGrath, and Alan Mackay-Sim

Background: Evidence from genetic association studies implicate genes involved in neural migration associated with schizophrenia risk. Neural stem/progenitor cell cultures (neurosphere-derived cells) from olfactory mucosa of schizophrenia patients have significantly dysregulated expression of genes in focal adhesion kinase (FAK) signaling, a key pathway regulating cell adhesion and migration. The aim of this study was to investigate whether olfactory neurosphere-derived cells from schizophrenia patients have altered cell adhesion, cell motility, and focal adhesion dynamics.

Methods: Olfactory neurosphere-derived cells from nine male schizophrenia patients and nine male healthy control subjects were used. Cells were assayed for cell adhesion and cell motility and analyzed for integrins and FAK proteins. Focal adhesions were counted and measured in fixed cells, and time-lapse imaging was used to assess cell motility and focal adhesion dynamics.

Results: Patient-derived cells were less adhesive and more motile than cells derived from healthy control subjects, and their motility was reduced to control cell levels by integrin-blocking antibodies and by inhibition of FAK. Vinculin-stained focal adhesion complexes were significantly smaller and fewer in patient cells. Time-lapse imaging of cells expressing FAK tagged with green fluorescent protein revealed that the disassembly of focal adhesions was significantly faster in patient cells.

Conclusions: The evidence for altered motility and focal adhesion dynamics in patient-derived cells is consistent with dysregulated gene expression in the FAK signaling pathway in these cells. Alterations in cell adhesion dynamics and cell motility could bias the trajectory of brain development in schizophrenia.

Key Words: Cell migration, disease model, neurodevelopment, patient-derived, schizophrenia, stem cell

Patients with schizophrenia have slight reductions in cortical thickness (1) and reductions in volume in several brain regions preceding the onset of the full clinical disorder (2). At the cellular level, postmortem studies have identified differences in the densities of neurons in the brains of schizophrenia patients compared with control subjects, such as increased numbers or densities of interstitial white matter neurons and reductions in interneurons in various cortical regions (3–9). It is suggested that neural migration is altered during brain development in schizophrenia (3,5), consistent with reduced reelin expression in the brain of schizophrenia patients (10). Genetic studies implicate genes involved in cell migration in schizophrenia; for example, well-described findings related to *DISC1* (disrupted in schizophrenia 1), *RELN* (reelin), and *NRG1* (neuregulin) converge on

mechanisms related to neuronal migration during brain development (4,11–13). Cell migration requires appropriate cell adhesion. Genome-wide association studies identified cell adhesion pathways to be over-represented among common single nucleotide polymorphisms in cases compared with control subjects (14,15). In vitro studies of patient-derived fibroblasts and olfactory mucosa biopsies showed reduced adhesion in schizophrenia (16–19). Collectively, these observations provide convergent evidence that cell adhesion pathways are potential contributors to altered neurodevelopment in schizophrenia, but understanding the cellular and molecular mechanisms that link genetics with functional deficits requires appropriate patient-derived cells.

The olfactory mucosa is accessible by biopsy in humans (20). It contains multipotent stem cells (21) and is capable of continuing neurogenesis of sensory neurons throughout adult life (22,23). Impaired olfactory identification is associated with schizophrenia (24). Therefore, as a regenerating neural tissue, the olfactory mucosa provides a relevant source of cells for investigating neurodevelopmental mechanisms of schizophrenia. This was demonstrated in patient-derived olfactory mucosa cultures showing more cell proliferation (18,19) and in patient-derived post-mortem samples of olfactory epithelium showing histological signs of altered neurogenesis (25). We developed a novel cell model on the basis of neural stem cells from olfactory mucosa biopsy from patients and healthy control subjects (“olfactory neurosphere-derived” [ONS] cells) (26,27). Cell proliferation was increased in these cells; they had a 2-hour shorter cell cycle; and cyclin D1 protein levels were elevated, indicating that there was dysregulation of the cell cycle (28). These patient-control differences were reflected in the prior analysis of gene expression in these cells that indicated significant dysregulation in expression of genes involved in G1/S phase checkpoint control (26). Among the 1700 genes that were differentially expressed in patient cells, there was a convergence of significantly altered gene expression in developmental pathways associated with cell adhesion, axon

From the National Centre for Adult Stem Cell Research (YF, GA, JYT, WM, AM-S), Eskitis Institute for Cell and Molecular Therapies, Griffith University; Australian Institute for Biotechnology and Nanotechnology (RM, JC-W); Queensland Brain Institute (JJM), The University of Queensland; Queensland Centre for Mental Health Research (JJM), The Park Centre for Mental Health, Brisbane, Queensland, Australia; and Programa de Biología Celular y Molecular (CCC, LL), Centro de Estudios Moleculares de la Célula, Instituto de Neurociencias Biomédicas, Instituto de Ciencias Biomédicas (ICBM), Facultad de Medicina, Universidad de Chile, Santiago, Chile.

Authors YF and GA contributed equally to this work.

Address correspondence to Alan Mackay-Sim, B.A. (Hons), Ph.D., National Centre for Adult Stem Cell Research, Griffith University, Kessels Rd, Brisbane, QLD 4111, Australia; E-mail: a.mackay-sim@griffith.edu.au.

Received Apr 23, 2012; revised and accepted Jan 15, 2013.

growth, and cell migration, including a large number in the “integrin adhesome” (29). Central to these related cell functions is the focal adhesion kinase (FAK) signaling pathway in which 33 genes were differentially expressed in patient cells (26). FAK signaling regulates the formation of focal adhesions (holding the cell onto the extracellular matrix) and the formation of actin stress fibers (providing the internal tension to drive cell morphology and migration). Focal adhesion complexes are large protein aggregates consisting of multiple structural and signaling components (30). These complexes are formed via integrin engagement, which link the intracellular cytoskeleton to the extracellular matrix, allowing the cells to integrate and respond to extracellular stimuli to adhere to the substrate and migrate through it (31). During brain development, cell migration requires adhesion to the extracellular matrix via integrins (32,33). The integrins are the cell membrane receptors for the extracellular matrix proteins. Two integrin genes (*ITGA8*, *ITGA3*) were among the focal adhesion signaling genes whose expression was altered in patient-derived cells compared with cells derived from healthy control subjects (26). It is notable that gene expression profiling of induced pluripotent cells derived from patient and control fibroblasts also identified cell adhesion as one of the dysregulated pathways in cells derived from schizophrenia patients (34). The aim of this study was to investigate whether ONS cells from schizophrenia patients have altered cell adhesion, cell motility, and focal adhesion dynamics.

Methods and Materials

Full details are provided in Supplement 1.

Cell Lines

The patient and control cells used here are those previously reported (26,28). Olfactory mucosa biopsies (18) were taken from nine male subjects with schizophrenia and nine healthy, age-matched control male subjects. Case-control status was determined with the Diagnostic Interview for Psychosis (35) according to criteria from the DSM-IV (36). Participant information is in Table 1. Biopsies were obtained with the written informed consent of the subjects, and the procedures were carried out in accordance with the ethics committees of The Park Centre for Mental Health and Griffith University, according to guidelines of the National Health and Medical Research Council of Australia.

Cell Culture

Olfactory neurosphere-derived cells derived from patients with schizophrenia are referred to as “Patient” cells. Cells derived from healthy control subjects are referred to as “Control” cells. Frozen aliquots of Patient and Control cells were thawed and grown as described previously (26). All assays were done with cells cultured for similar periods after nasal biopsy (between 5 and 8 passages from the initial plating). The ONS cells derived from patients and control subjects have similar morphologies, with similar proportions of cells expressing the different antigens representative of markers for bone marrow stromal cells, neural stem cells, neurons, and glia (Table S1 in Supplement 1) (26).

Protein Analysis

The proportion of cells immuno-stained with anti-integrin $\beta 1$ and anti-integrin $\alpha 3$ were quantified with flow cytometry. Protein extracts from cell lysates were analyzed with enzyme-linked

Table 1. Participant Details

Cell Line ID	Age	Sex	Medication	CPE	Cigarettes/Day
Control Subjects					
10002001	31	Male			
10002002	47	Male			10
10002003	28	Male			
10003001	17	Male			
10003002	24	Male			
10003003	32	Male			
10003004	46	Male			
10003005	56	Male			
10003006	45	Male			5
Patients					
30002001	46	Male	Clozapine: 250 mg/day Omeprazole magnesium: 20 mg/day	333	25
30002002	58	Male	Olanzapine: 7.5 mg/day Benztropine: 1 mg/day Diclofenac sodium: 100 mg/day	250	
30002003	21	Male	Quetiapine: 800 mg/day Paroxetine: 40 mg/day	1194	15
30002004	33	Male	Risperidone: 4 mg/day	267	
30002005	49	Male	Clozapine: 350 mg/day	467	
30002006	27	Male	Olanzapine: 16 mg/day	533	30
30002007	44	Male	Clozapine: 475 mg/day Lithium Carbonate: 1250 mg/day Atenolol: 75 mg/day Aspirin: Dose unknown	633	20
30002008	28	Male	Flupenthixol decanoate: 200 mg/month	500	10
30002009	38	Male	Risperidone: Dose unknown	unknown	60

Chlorpromazine equivalent (CPE) medication dose, calculated according to Davis (41). Data from Matigian *et al.* (26).

immunosorbent assay kits according to the manufacturer's instructions: FAK (STAR FAK ELISA Kit; Millipore Catalog number 17-479 [Millipore, Billerica, Massachusetts]; measured in nanograms/milligram protein) and phosphorylated focal adhesion kinase (pFAK) (Y397-pFAK; STAR pFAK ELISA Kit; Millipore Catalog number 17-480; measured in units/milligram [U/mg] protein).

Cell Adhesion

Cells were seeded on fibronectin-coated wells and allowed to attach for 2 hours; then unattached cells were washed off, and attached cells were quantified by DNA content. Relative attachment of cells was obtained by normalizing to the control group mean.

Cell Migration–Barrier Assay

Cells were seeded within a ring-device in fibronectin-coated plates and allowed to attach for 4 hours to obtain a confluent monolayer, after which the device was removed and the non-adherent cells were washed off. The cells were then allowed to migrate away from the central region for 72 hours. After fixation cell nuclei were counted with Image J software (37) and the proportion of cells migrating from the central region was calculated. Because Patient and Control cells have differential rates of cell proliferation (28), which would affect cell numbers, cell proliferation was prevented by adding 5-fluorouracil (10 $\mu\text{g}/\text{mL}$) to the medium. A control experiment was performed without 5-fluorouracil in the medium.

Cell Migration-Microfluidics Assay

Cell migration was investigated with a microfluidic assay in a multichannel migration device that allows reproducible and easy quantification of cell motility (37). The device consists of a main chamber with 200- μm -wide migration channels protruding perpendicularly from it. Cell proliferation was prevented by synchronizing cell cycles in G1 before the assay (28). Synchronized cells were seeded for 4 hours in the fibronectin-coated main chamber to establish a confluent monolayer, after which non-adherent cells were washed away, and the migration channels were backfilled with media to break the fluid meniscus that otherwise prevents medium from flowing from the main chamber into the migration channels. Images were taken at 0 and 20 hours, and the furthest distance travelled by the cells was measured in each microchannel with Image J software (37). FAK phosphorylation was inhibited with FAK Inhibitor 14 (FAK In14). In pilot studies, 3 $\mu\text{mol}/\text{L}$ FAK In14 was nontoxic to the cells and blocked migration (Figure S1 in Supplement 1). The activity of FAK In14 was confirmed by Western analysis of protein samples of treated and untreated cells (Figure S2 in Supplement 1). Integrin activity was reduced by pre-incubating cells for 1 hour with antibodies against integrin $\alpha 3$, integrin $\alpha 8$, and integrin $\beta 1$. The FAK In14 and blocking antibodies were present in the medium before seeding and throughout the assay period.

Quantitative Microscopy for Cell Tracking and Focal Adhesion Complex Dynamics

Cells were transiently transfected with plasmid encoding green fluorescent protein (GFP)-FAK (kindly donated by Mike Schaller) (38). After transfection, cells were grown for 24 hours and then visualized in a confocal microscope, and motility was quantified in time-lapse videos by tracking the coordinates of the center of the nucleus in each frame at intervals of 10 min for 48 hours. The disassembly period of individual focal adhesions was calculated from time-lapse images of GFP-FAK cells, acquired

every 1 min for 90 min at 37°C at 400 \times magnification. Focal adhesion disassembly was visualized and quantified manually as the loss of fluorescence of each individual, fully formed structure. Focal adhesions start as focal points that elongate slowly over time. They are found at both ends of actin stress fibers from cell periphery to the perinuclear region. They are considered focal adhesions when they meet the following criteria: area (1–10 μm^2), shape (elongated), and location (cell periphery or perinuclear) (30). Focal adhesion disassembly was determined from the time elapsed between those frames in which a fully formed focal adhesion, which stopped growing, was observed to disappear. Thus, if a focal adhesion stopped growing at frame number 30 and disappeared at frame number 60, then the focal adhesion took 30 min to disassemble. Sequential video images were processed with Imaris software (Bitplane, Zurich, Switzerland) [see also Goetz *et al.* (39)].

Quantification of the Number and Size of Focal Adhesions

Cells were grown for 24 hours, and immunofluorescence was performed for vinculin immunoreactivity (40). The number of focal adhesions/cell and the average area of these focal adhesions were visualized by confocal microscopy and quantified with Image J and the plug-in "Analyse particles" (<http://rsbweb.nih.gov/ij/docs/menus/analyze.html>). Focal adhesions were selected as structures of determined pixel range above the threshold (background) value (40). Numbers were obtained from 7 to 10 cells/patient ($n = 3$) and control ($n = 3$) individuals.

Effects of Medication and Smoking

Medication dose, as chlorpromazine dose equivalents (41), and smoking (cigarettes/day; Table 1) were correlated with pFAK levels (Figure 1A), cell attachment (Figure 1B), barrier migration assay (Figure 2A), microchannel device assay (Figures 2B and 3), and percentage of cells expressing integrins $\alpha 3$ and $\beta 1$.

Statistical Analysis

Data are expressed as mean \pm SEM. The statistical programs SPSS 20.0 (SPSS, Chicago, Illinois) and GraphPad Prism 5.01 (GraphPad, San Diego, California) were used to compare the measurements of interest between the Patient and Control cells (analysis of variance [ANOVA], *t* test, 2-tailed, Pearson product moment correlation coefficient). The effects of smoking were analyzed with general linear models (statistical program SAS; SAS Institute, Cary, North Carolina), and the effect of medication dose was evaluated with Spearman correlation (SAS). Statistical differences were considered significant as $\alpha < .05$.

Results

Patient Cells Had Less pFAK

There was no difference in levels of total FAK in Patient and Control cells (Control: 398 \pm 32 ng/mg protein; Patient: 373 \pm 19 ng/mg protein; $p = .51$). In contrast, the level of pFAK in Patient cells was significantly less than in Control subjects (Figure 1A). The mean levels of pFAK were: Control, 22.36 \pm 1.79 U/mg protein, $n = 9$; Patient, 10.71 \pm 1.68 U/mg protein, $n = 9$ [$F_{1,16} = 22.56$, $p < .001$].

Patient Cells Expressed Integrins $\alpha 3$ and $\beta 1$

Patient cells and Control cells expressed $\alpha 3$ and $\beta 1$ integrins. Slightly fewer Patient cells expressed $\alpha 3$ integrin compared with Control subjects (integrin $\alpha 3$: 95.6% \pm .81 and 98.3% \pm .20,

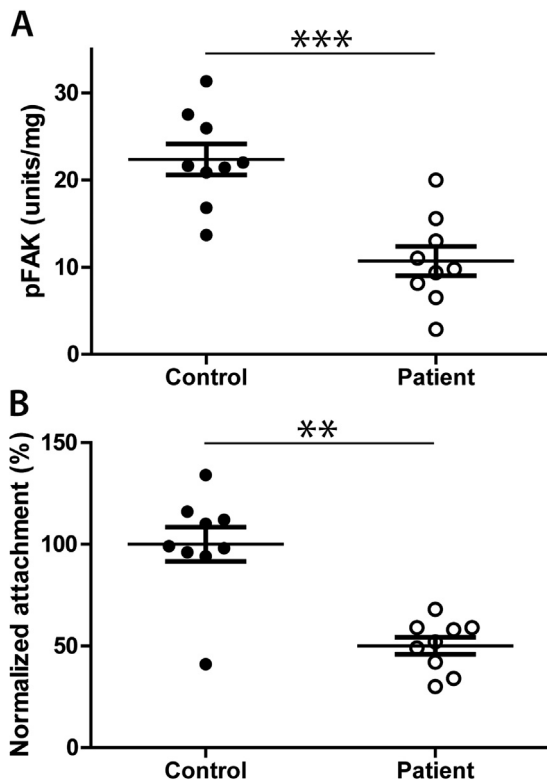


Figure 1. Patient cells had less phosphorylated focal adhesion kinase (pFAK) and were less adhesive. **(A)** The pFAK content in Patient and Control cells measured by enzyme-linked immunosorbent assay. The pFAK content (mean \pm SEM) was significantly less in Patient cells (open circles) than Control cells (closed circles). (***) $p < .001$. **(B)** Proportion of cells adherent 120 min after plating on fibronectin, expressed relative to the average of the Control cells. Adhesion (mean \pm SEM) was significantly less for Patient cells (open circles) than Control cells (closed circles) (** $p < .01$).

respectively; $p = .007$; integrin $\beta 1$: $93.8\% \pm 2.3$ vs. $97.0\% \pm .6$; $p = .193$).

Patient Cells Were Less Adherent Than Control Cells

Differential cell adhesion was measured by quantifying the proportion of cells attached to the fibronectin substrate 2 hours after seeding. Significantly fewer Patient cells remained attached to the fibronectin substrate (Figure 1B) [$t_{16} = 5.3$, $p = .0001$; $n = 9$ cell lines/group].

Patient Cells Were More Motile Than Control Cells

In the barrier assay after 72 hours, significantly more Patient cells migrated out of the central region into surrounding regions (Figure S2 in Supplement 1; Figure 2A) [$t_{68} = 2.7$, $p = .008$; $n = 9$ cell lines/group, 4 replicates/cell line]. Cells were treated with 5-fluorouracil to block proliferation. In the absence of 5-fluorouracil, significantly more Patient cells migrated out of the central region compared with Control cells [Control: 6435 ± 956 ; Patient: $13,400 \pm 2832$; $t_{14} = 2.3$, $n = 8$ cell lines/group]. These numbers are confounded by cell proliferation, because Patient cells proliferated more rapidly than Control subjects (28). This confound was eliminated in the microchannel migration device, not with 5-fluorouracil but by synchronizing the cell cycle before the assay and examining cells at 20 hours, less than the cell cycle period. In the microchannel migration device, Patient cells moved

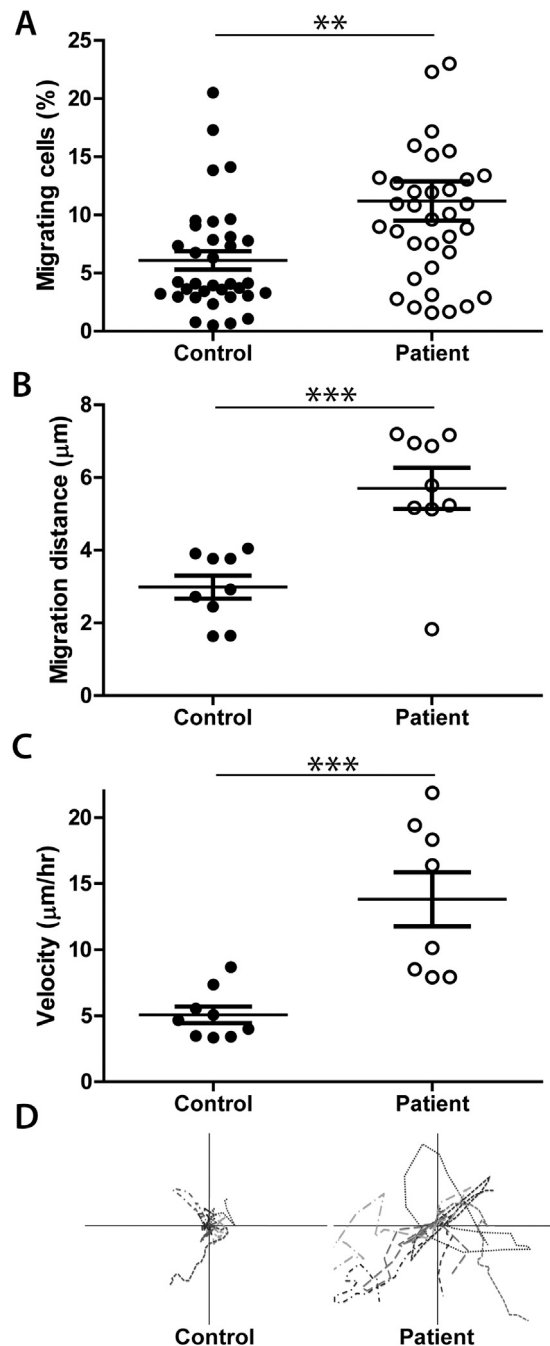


Figure 2. Patient cells were more motile than Control cells. **(A)** Percentage of cells migrating away from the central well in the barrier assay over 72 hours. Significantly more Patient cells moved out of the central area. The migration distance (mean \pm SEM) was significantly further for Patient cells (open circles) than Control cells (closed circles). All replicate experiments are shown (** $p < .01$). **(B)** The distance moved by cells in 20 hours in the microchannel migration device. The migration distance (mean \pm SEM) was significantly further for Patient cells (open circles) than Control cells (closed circles) (***) $p < .001$. **(C)** The velocity of movement during 24 hours with time-lapse imaging. The migration speed (mean \pm SEM) was significantly faster for Patient cells (open circles) than Control cells (closed circles) (***) $p < .001$. **(D)** Individual tracks of cell movement during 24 hours with time-lapse imaging. Tracks of individual cells are shown with different lines, with the origin of the axis as the start point for each cell. Velocity was calculated from the length of each line divided by time.

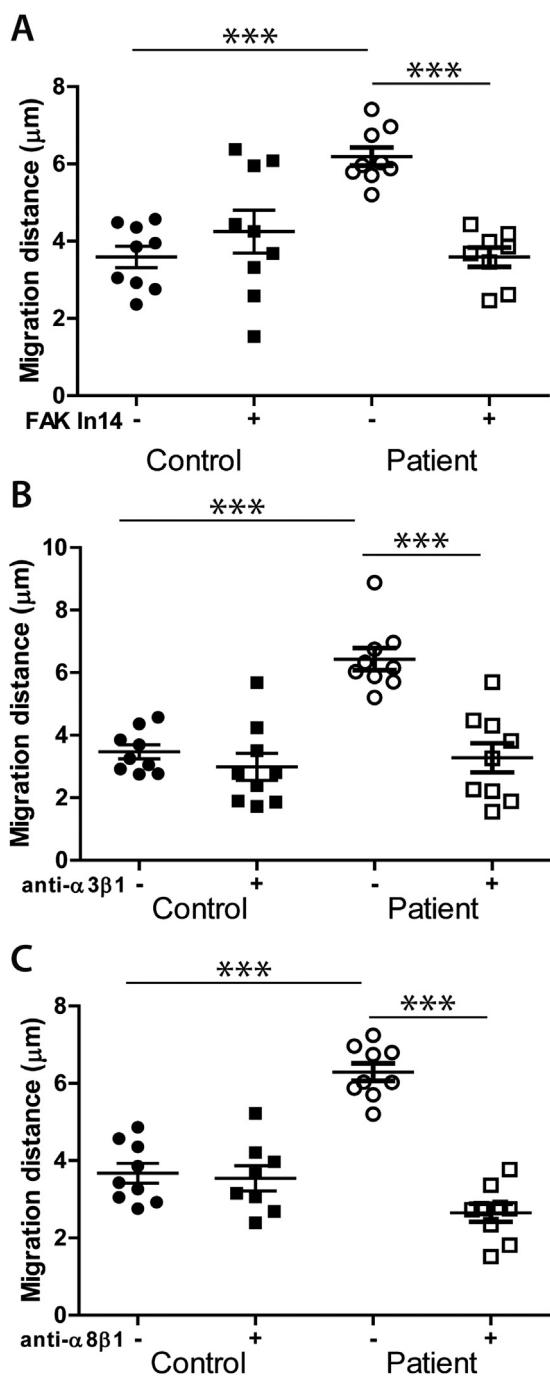


Figure 3. Patient cell motility was reduced by blocking focal adhesion kinase (FAK) and integrin binding. The distance moved by cells in 24 hours in the microchannel migration device. The graphs show mean \pm SEM for Patient cells (open symbols) and Control cells (closed symbols): with FAK In14 (squares) and without (circles) (A); with antibodies to $\alpha 3\beta 1$ integrins (squares) and without (circles) (B); and with antibodies to $\alpha 8\beta 1$ integrins (squares) and without (circles) (C). Untreated Patient cells migrated further than Control cells ($t = 5.04$, $***p < .0001$; Bonferroni corrected). Inhibition of focal adhesion kinase activity significantly reduced Patient cell migration ($t = 4.89$, $***p < .0001$), as did antibodies to $\alpha 3\beta 1$ integrins ($t = 5.65$, $***p < .0001$) and $\alpha 8\beta 1$ integrins ($t = 6.87$, $***p < .0001$).

significantly further than Control cells (Figure S2 in Supplement 1; Figure 2B) [$t_{18} = 4.2$, $p = .0007$]. The barrier assay and microchannel device quantify motility of cell populations; the velocity

of movement of individual Patient and Control cells was recorded with time-lapse imaging. Patient cells moved significantly faster than Control cells (Figure 2C) [$t_{15} = 4.3$, $p = .0006$]. Patient cells moved 2.6-fold faster than Control cells, but the trajectories of cells in both groups were essentially random and not directional (Figure 2D). Noteworthy, cell tracks of Patient cells reflect that these cells move faster and farther than Control cells (Figure 2D).

Patient Cell Motility Was Sensitive to Inhibition of FAK and Integrin Binding

Cell motility was quantified with and without pFAK inhibition. In the absence of FAK In14, the Patient cells migrated further than Control cells, but this difference was eliminated by the inhibitor (Figure 3A). The FAK inhibition did not affect the basal migration rate of Control cells (Figure 3A). A pilot study of three Patient cells and three Control cells demonstrated that blocking antibodies to integrins $\alpha 8$ and $\beta 1$ reduced the motility of Patient cells (Figure S3 in Supplement 1). The experiment was repeated with all cell lines confirming that integrin antibodies to $\alpha 3$ and $\beta 1$ as well as $\alpha 8$ and $\beta 1$ reduced the motility of the Patient cells without affecting Control cells (Figure 3B and C). Repeated measures ANOVA demonstrated a significant effect of treatment [$F_{3,61} = 12.07$, $p < .0001$] and a significant treatment \times disease status interaction [$F_{3,61} = 11.29$, $p < .0001$]. Subsequent individual repeated measures ANOVA of the Patient and Control cell data indicated a significant treatment effect for the Patient cells [$F_{3,21} = 25.18$, $p < .0001$] but not the Control cells [$F_{3,21} = 2.67$, $p = .07$]. Post hoc Bonferroni corrected t tests indicated that the motility of untreated Patient cells were significantly different from treated Patient cells and from untreated Control cells, which were not different from the treated Control cells.

Cell Motility Was Correlated with pFAK Levels and Adhesion

For each cell line, the migration distance was averaged for the four assays in the microchannel migration device (uninhibited) (Figures 2B and 3A–C). These values were then plotted for each individual against pFAK (units/milligram) (Figure 1A) and adhesion (percentage attached after 120 min) (Figure 1B). Migration distance was negatively correlated with pFAK levels ($r = -.61$, $p = .007$) (Figure 4A) and adhesion ($r = -.712$, $p = .0009$) (Figure 4B).

No Effects of Medication or Smoking

Patient medications and doses were converted into chlorpromazine equivalents (41). There were no significant associations between chlorpromazine equivalents and any of the migration-related outcomes (pFAK, percentage attachment, percentage of cells migrating in barrier assay, migration distance in microchannel migration device, percentage of cells expressing integrin $\beta 1$ and $\alpha 3$; Spearman $\rho > .05$ for all comparisons). Patients were more likely to be smokers compared with control subjects (5 of 9 patients compared with 2 of 9 control subjects). Thus, to examine the association between cigarette use (assessed as average number of cigarettes/day) and the key cell migration-related variables, we use general linear models. When adjusted for case status, there were no significant associations between cigarette use and any of the outcome variables ($p > .05$).

Patient Cells Had Fewer and Smaller Focal Adhesions

Focal number and size were quantified from vinculin immunofluorescence (Figure 5A,B). Patient cells had significantly fewer focal adhesions than Control cells (Figure 5C) [19 ± 2.6 vs. 29 ± 3 , $t_{37} = 2.3$, $p = .024$]. Patient cell adhesions were

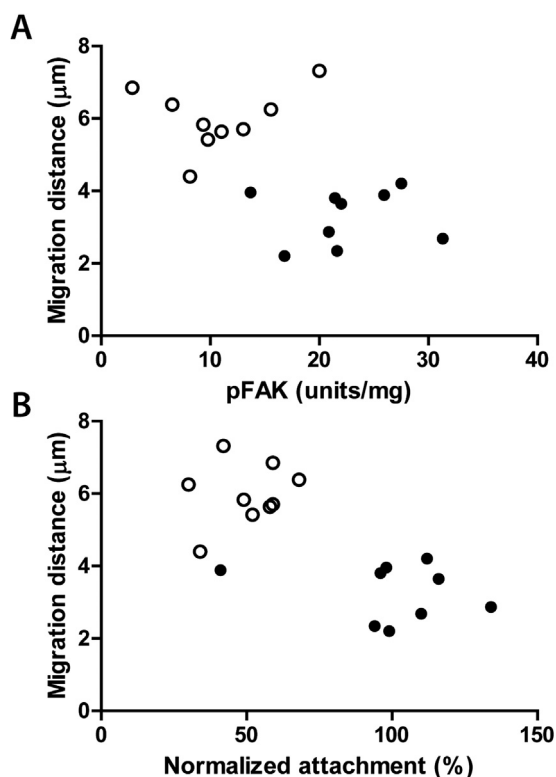


Figure 4. Cell motility was correlated with phosphorylated focal adhesion kinase (pFAK) levels and adhesion. **(A)** Migration distance of all cell lines (averaged from Figures 2B and 3A–C) plotted against pFAK levels (Figure 1A); $r = -.61$, $p = .007$. **(B)** Migration distance of all cell lines (averaged from Figures 2B and 3A–C) plotted against normalized attachment (Figure 1B); $r = -.71$, $p = .0009$. Patient cells, open circles; Control cells, closed circles.

significantly smaller than Control cell adhesions (Figure 5D) [$5.0 \pm .38$ vs. $7.1 \pm .50$, $t_{37} = 3.5$, $p = .0012$]. Focal adhesion “mass” was estimated from the product of average number and area. Control cells had twice the mass of Patient cells (206 vs. 95).

Patient Cell Focal Adhesions Disassembled Faster

Focal adhesion disassembly dynamics were quantified in cells expressing GFP-FAK (Figure 6; Supplement 2 and Supplement 3). The time taken to disassemble focal adhesions was quantified from the video frame showing maximum size until disappearance of the adhesion (Figure 6A,B). Patient cell adhesions disassembled significantly faster than Control cell adhesions, with disassembly occurring after 32 ± 3.6 min and 56 ± 3.7 min, respectively (Figure 6) [$t_{38} = 20.8$, $p < .0001$].

Discussion

These experiments show that ONS cells from schizophrenia patients have reduced cell adhesion and increased cell motility that is associated with dysregulated FAK phosphorylation and altered focal adhesion dynamics. Patient cells had less Y397-pFAK compared with Control cells, and their motility was reduced to Control levels by a small molecule inhibitor of FAK. Blocking antibodies to $\alpha 8$ - and $\beta 1$ -integrins also reduced Patient cell motility to Control levels. The ONS cells used in this analysis are the same as those used previously (26,28) and examined after similar periods in vitro. There are no obvious differences in Patient and Control cell populations, with respect to each other,

although there is heterogeneity within them. Olfactory neurosphere-derived cells are morphologically undifferentiated, and most express some antigens associated with bone marrow stromal cells (CD105, CD73), with smaller percentages expressing markers of neural stem cells (nestin) and neural progenitors (β -tubulin-III) (26). They have been called “ecto-mesenchymal” stem or progenitor cells (42). As discussed previously (26,28), prior medication, treatment, or lifestyle factors might contribute to disease-associated differences in these cells, but in the present study, Patient-Control differences were not explained by correlation with antipsychotic medication or smoking.

Focal adhesions provide the link between cell attachment, detachment, and migration, whereby decreased strength of focal adhesions is associated with greater cell motility (30,43). Cell motility is enhanced by manipulations that decrease the size and number of focal adhesions (44). In agreement with this, Patient cells had half the size and number of focal adhesions and twice the motility of Control cells and half the time of disassembly. The faster disassembly in Patient cells can account for their smaller focal adhesions. These observations suggest that the differences in motility of Patient and Control cells are related to the dynamics of focal adhesion assembly/disassembly.

FAK is central to neuronal migration (45,46) and is a hub in the focal adhesion complex that forms and disassembles to mediate cell binding to the extracellular matrix (47). Y397-pFAK, the autophosphorylated form examined here, is essential for the subsequent FAK phosphorylations that initiate integrin-mediated cell adhesion and is present in newly forming and mature focal adhesions (48). Thus, the maximum measured level of pFAK is limited to the amount aggregated in focal adhesion complexes. Patient cells have half the pFAK level and hence half the focal adhesion mass compared with Control cells, consistent with being less adhesive and more motile. Surprisingly, reduction of pFAK in Patient cells reduced motility to Control levels. Several explanations are possible, but more experimental evidence is required to choose among mechanistic interpretations of these paradoxical results. They might reflect the cyclic nature of the migration process (49). For instance, tyrosine phosphatases regulate disassembly of focal adhesions (50), and lower baseline levels of Y397-pFAK in Patient cells could indicate more active tyrosine phosphatases. Hence, FAK autophosphorylation and phosphatase-driven dephosphorylation might be more rapid in Patient cells and further FAK inhibition might no longer support dynamic turnover of pFAK, thereby reducing motility. A different possibility is that the baseline Patient-Control difference in pFAK levels could result from differences in expression of genes other than FAK. Factors that regulate integrin expression and activity could contribute, because adhesion strength is exponentially dependent on the number of integrin molecules bound to the focal adhesion (51). Numerous genes, both upstream and downstream of FAK phosphorylation, have dysregulated expression in Patient cells (26), so it is difficult to identify the primary deficit in these cells. For example, “ErbB signaling” and “Ephrin receptor signaling” are dysregulated in Patient cells (26). Inhibition of ErbB2 enhances the number and size of focal adhesions and inhibits cell motility (52), and EphA2 activation inactivates integrins to inhibit cell motility (52).

Patient cell motility was dependent on integrin engagement, indicated by blocking antibodies to $\alpha 8$ and $\beta 1$ integrins, which dimerize to bind to fibronectin (53). Integrins are the primary cell membrane receptors for focal adhesion signaling, mediating interactions between cells and extracellular matrix (30). Integrin receptors are heterodimers between many combinations of α

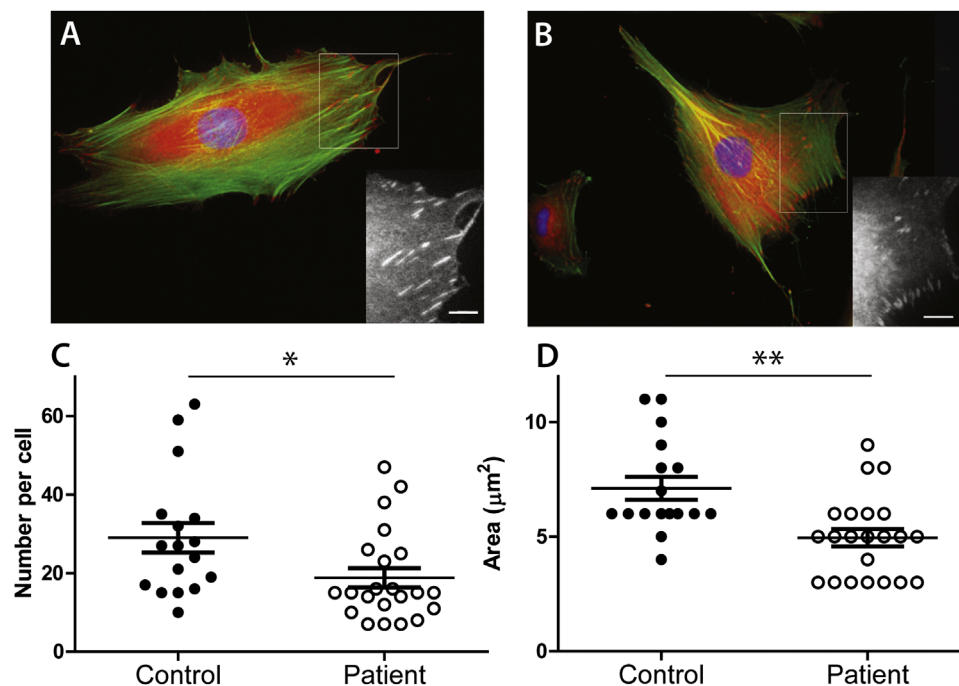


Figure 5. Patient cell focal adhesions were fewer and smaller. Examples of focal adhesions in Control cells (A) and Patient cells (B). Note that in Patient cells many spots are focal points (smaller, round) and not focal adhesions (larger, elongated). Focal adhesions (red) were stained with an antivinculin monoclonal antibody, followed by Alexa Fluor 546 antimouse IgG (Invitrogen, Carlsbad, California). Actin stress fibers (green) were stained with Alexa Fluor 488-conjugated phalloidin. Nuclei (blue) were stained with 4',6-diamidino-2-phenylindole (DAPI) and visualized with an Olympus IX70 inverted microscope (Olympus, Melville, New York). Insets represent magnified views of focal adhesions in the selected regions of interest. Scale bars = 10 μm . (C) The number of focal adhesions/cell (mean \pm SEM) for Patient cells (open circles) and Control cells (closed circles) ($n = 20$ cells from 3 cell lines/group). Patient cells had significantly fewer adhesions than Control cells (* $p < .05$). (D) The average area of focal adhesions/cell (mean \pm SEM) for Patient cells (open circles) and Control cells (closed circles) ($n = 20$ cells from 3 cell lines/group). Patient cells had significantly smaller adhesions than Control cells (** $p < .01$).

and β subunits, which account for their multiple ligand specificities (53). As reported previously (26), Patient cells expressed significantly less integrin $\alpha 3$ messenger RNA (mRNA) and significantly more $\alpha 8$ mRNA than Control cells. Integrin $\alpha 8$ is a receptor subunit for fibronectin, osteopontin, and tenascin; and integrin $\alpha 3$ is a receptor subunit for laminin, reelin, and thrombospondin (53). Fittingly, mRNA for two subunits of laminin and two members of the thrombospondin family were significantly over-expressed in Patient cells (Table S2 in Supplement 1) (26). Therefore, Patient cells might be differentially adhesive on multiple substrates, although this remains to be confirmed. Motility of Control cells was unaffected by FAK inhibition and integrin blockade, presumably because at baseline they were relatively non-motile on fibronectin, having more, larger, and less dynamic focal adhesions. The FAK inhibitor diminished the motility of Patient cells to the same basal levels observed in Control cells, indicating that the signaling pathways activated to maintain this background state of motion are less sensitive to integrin binding levels and FAK phosphorylation.

The present study draws attention to FAK signaling as a potential candidate pathway that could affect neuronal migration in the developing brain in schizophrenia, sharing certain attributes with *RELN* (54), *DISC1* (55), and *NRG1* (56) pathways. For example, genetic deletions of *FAK* and integrin $\alpha 3$ lead to defects in laminations of the cerebral cortex similar to deletions of *RELN*, *DISC1*, and *NRG1* (57–61). Focal adhesion kinase is strongly expressed in the developing and adult brain, enriched in cerebral and cerebellar cortices and hippocampus (62). Deletion of the *FAK* gene is embryonic lethal in mouse, but cell-specific deletions

provide insights into its role in brain development (59). Deletion of FAK in glia and meningeal fibroblasts cause dysgenesis of the frontal cortex, apparently by disrupting the attachment of radial glia end-feet to the basal lamina, generated by meningeal fibroblasts, thereby indirectly impairing neuronal migration and cortical lamination (59). Neuron-specific deletion of FAK did not affect cortical lamination but reduced neuritogenesis and axon path-finding (59). Genetic deletion of integrin $\alpha 3$ disrupts cortical lamination, consistent with a neuronal migration deficit during development (58). Mouse studies demonstrate multiple tissue-specific roles for integrins during development (63), including in neuronal migration and lamination of the cerebral cortex (58,64). Patient-control differences in FAK signaling are also relevant to increased cell proliferation in patient ONS cells (28). Patient cells had disrupted gene regulation of G1/S-phase transition (26), a shorter cell cycle period, and raised levels of cyclin D1, indicating that the raised cyclin D1 levels were driving the shorter cell cycle and increased proliferation rate (28). Over-expression of FAK modulates cell cycle dynamics by stimulating the expression of cyclin D (65), so it is plausible that the increased cyclin D1 levels and higher proliferation rate in Patient cells might be downstream of dysregulated FAK signaling in these cells. Pathway analysis of large genome-wide association datasets identified “focal adhesion” (14) and “cell adhesion molecule” (15) as signaling pathways with significant over-representation of single nucleotide polymorphisms in the patient cohorts. Additionally, when a gene identified through genome-wide association in schizophrenia (*ZNF804A*) was manipulated in neural progenitor cells, the expression of cell adhesion genes were specifically

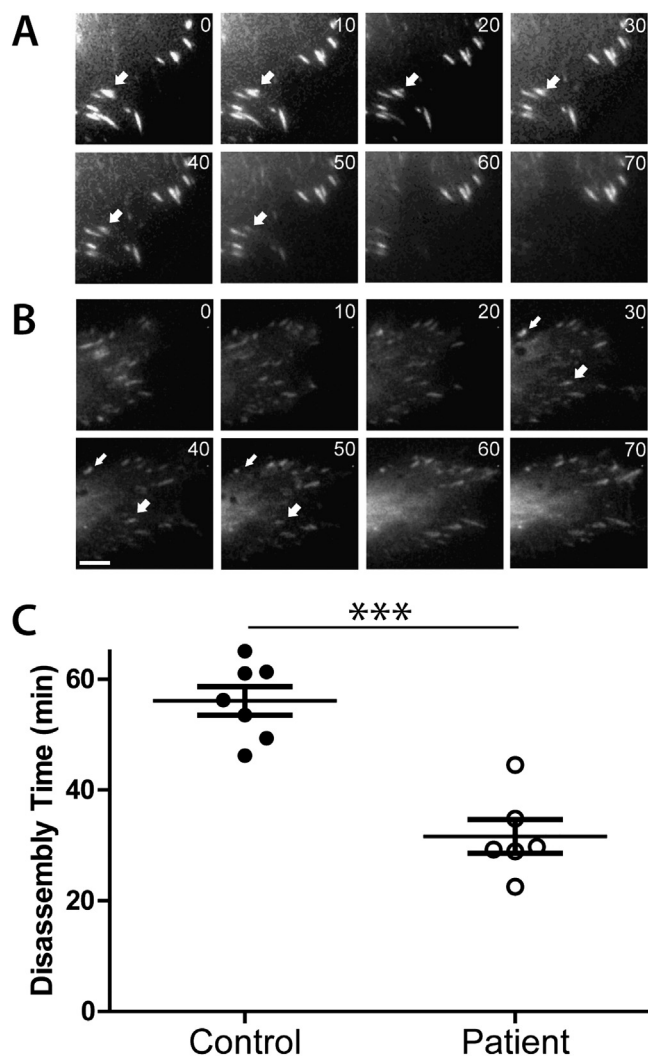


Figure 6. Patient cells disassembled focal adhesions faster than Control cells. Examples of focal adhesions from Control (A) and Patient cells (B) expressing green fluorescent protein-FAK taken every 10 min for 70 min, as indicated. When a focal adhesion stops growing, it is considered “mature” or fully formed; this is taken as the beginning of disassembly. The disappearance of the focal adhesion determines the end of the disassembly period. The arrows point to adhesions undergoing disassembly. Scale bar = 20 μ m. (C) Focal adhesion disassembly kinetics were measured for at least 12 structures from each cell. The period of focal adhesion disassembly (mean \pm SEM) of Patient cell adhesions (open circles) was significantly faster than Control cell adhesions (closed circles) (** $p < .001$).

altered (66). These genetic studies indicate that gene polymorphisms in cell adhesion pathways might be upstream of the gene expression and functional differences observed in Patient and Control cells.

It is not possible to predict how brain development would be affected by the findings reported here. The extracellular environment of the developing brain is a three-dimensional structure involving much greater complexity of extracellular matrix, cells, and signaling molecules. In the developing brain there would be homeostatic regulation at the cellular, network, and systems levels that is absent *in vitro*. Nonetheless it is likely that the alterations in cell biology demonstrated here would bias homeostatic regulation, potentially making it more susceptible to other

genetic or environmental stressors, thereby altering the trajectory of brain development.

The project was funded by a grant from the Australian Government Department of Health and Ageing, along with partial funding from the Australian Research Council Discovery Grants Scheme (DP110104446). LL is supported by FONDECYT 1110149; Award Number R03TW007810 from the Fogarty International Center, National Institutes of Health; *Iniciativas Científicas Milenio: Biomedical Neuroscience Institute P09-015-F; Anillos ACT1111.*

The authors report no biomedical financial interests or potential conflicts of interest.

Supplementary material cited in this article is available online at <http://dx.doi.org/10.1016/j.biopsych.2013.01.020>.

- Goldman AL, Pezawas L, Mattay VS, Fischl B, Verchinski BA, Chen Q, *et al.* (2009): Widespread reductions of cortical thickness in schizophrenia and spectrum disorders and evidence of heritability. *Arch Gen Psychiatry* 66:467–477.
- Vita A, De Peri L, Silenzi C, Dieci M (2006): Brain morphology in first-episode schizophrenia: A meta-analysis of quantitative magnetic resonance imaging studies. *Schizophr Res* 82:75–88.
- Yang Y, Fung SJ, Rothwell A, Tianmei S, Weickert CS (2011): Increased interstitial white matter neuron density in the dorsolateral prefrontal cortex of people with schizophrenia. *Biol Psychiatry* 69:63–70.
- Eastwood SL, Harrison PJ (2003): Interstitial white matter neurons express less reelin and are abnormally distributed in schizophrenia: Towards an integration of molecular and morphologic aspects of the neurodevelopmental hypothesis. *Mol Psychiatry* 8:769, 821–731.
- Akbarian S, Kim JJ, Potkin SG, Hetrick WP, Bunney WE Jr, Jones EG (1996): Maldistribution of interstitial neurons in prefrontal white matter of the brains of schizophrenic patients. *Arch Gen Psychiatry* 53:425–436.
- Benes FM, McSparren J, Bird ED, SanGiovanni JP, Vincent SL (1991): Deficits in small interneurons in prefrontal and cingulate cortices of schizophrenic and schizoaffective patients. *Arch Gen Psychiatry* 48:996–1001.
- Guidotti A, Auta J, Chen Y, Davis JM, Dong E, Gavin DP, *et al.* (2011): Epigenetic GABAergic targets in schizophrenia and bipolar disorder. *Neuropharmacology* 60:1007–1016.
- Kalus P, Senitz D, Beckmann H (1997): Cortical layer I changes in schizophrenia: A marker for impaired brain development? *J Neural Transm* 104:549–559.
- Arnold SE, Hyman BT, Van Hoesen GW, Damasio AR (1991): Some cytoarchitectural abnormalities of the entorhinal cortex in schizophrenia. *Arch Gen Psychiatry* 48:625–632.
- Fatemi SH (2005): Reelin glycoprotein: Structure, biology and roles in health and disease. *Mol Psychiatry* 10:251–257.
- Sei Y, Ren-Patterson R, Li Z, Tunbridge EM, Egan MF, Kolachana BS, *et al.* (2007): Neuregulin1-induced cell migration is impaired in schizophrenia: Association with neuregulin1 and catechol-o-methyltransferase gene polymorphisms. *Mol Psychiatry* 12:946–957.
- Seshadri S, Kamiya A, Yokota Y, Prikulis I, Kano S, Hayashi-Takagi A, *et al.* (2010): Disrupted-in-Schizophrenia-1 expression is regulated by beta-site amyloid precursor protein cleaving enzyme-1-neuregulin cascade. *Proc Natl Acad Sci U S A* 107:5622–5627.
- Fatemi SH, Folsom TD (2009): The neurodevelopmental hypothesis of schizophrenia, revisited. *Schizophr Bull* 35:528–548.
- Weng L, Maciardi F, Subramanian A, Guffanti G, Potkin SG, Yu Z, *et al.* (2011): SNP-based pathway enrichment analysis for genome-wide association studies. *BMC Bioinformatics* 12:99.
- O’Dushlaine C, Kenny E, Heron E, Donohoe G, Gill M, Morris D, *et al.* (2011): Molecular pathways involved in neuronal cell adhesion and membrane scaffolding contribute to schizophrenia and bipolar disorder susceptibility. *Mol Psychiatry* 16:286–292.
- Mahadik SP, Mukherjee S, Wakade CG, Laev H, Reddy RR, Schnur DB (1994): Decreased adhesiveness and altered cellular distribution of fibronectin in fibroblasts from schizophrenic patients. *Psychiatry Res* 53:87–97.
- Miyamae Y, Nakamura Y, Kashiwagi Y, Tanaka T, Kudo T, Takeda M (1998): Altered adhesion efficiency and fibronectin content in

- fibroblasts from schizophrenic patients. *Psychiatry Clin Neurosci* 52: 345–352.
18. Feron F, Perry C, Hirning MH, McGrath J, Mackay-Sim A (1999): Altered adhesion, proliferation and death in neural cultures from adults with schizophrenia. *Schizophr Res* 40:211–218.
 19. McCurdy RD, Feron F, Perry C, Chant DC, McLean D, Matigian N, *et al.* (2006): Cell cycle alterations in biopsied olfactory neuroepithelium in schizophrenia and bipolar I disorder using cell culture and gene expression analyses. *Schizophr Res* 82:163–173.
 20. Feron F, Perry C, McGrath JJ, Mackay-Sim A (1998): New techniques for biopsy and culture of human olfactory epithelial neurons. *Arch Otolaryngol Head Neck Surg* 124:861–866.
 21. Murrell W, Feron F, Wetzig A, Cameron N, Splatt K, Bellette B, *et al.* (2005): Multipotent stem cells from adult olfactory mucosa. *Dev Dyn* 233:496–515.
 22. Hahn CG, Han LY, Rawson NE, Mirza N, Borgmann-Winter K, Lenox RH, *et al.* (2005): In vivo and in vitro neurogenesis in human olfactory epithelium. *J Comp Neurol* 483:154–163.
 23. Murrell W, Bushnell GR, Livesey J, McGrath J, MacDonald KP, Bates PR, *et al.* (1996): Neurogenesis in adult human. *Neuroreport* 7:1189–1194.
 24. Turetsky BI, Hahn CG, Arnold SE, Moberg PJ (2009): Olfactory receptor neuron dysfunction in schizophrenia. *Neuropsychopharmacology* 34: 767–774.
 25. Arnold SE, Han LY, Moberg PJ, Turetsky BI, Gur RE, Trojanowski JQ, *et al.* (2001): Dysregulation of olfactory receptor neuron lineage in schizophrenia. *Arch Gen Psychiatry* 58:829–835.
 26. Matigian N, Abrahamsen G, Sutharsan R, Cook AL, Vitale AM, Nouwens A, *et al.* (2010): Disease-specific, neurosphere-derived cells as models for brain disorders. *Dis Model Mech* 3:785–798.
 27. Mackay-Sim A (2012): Concise review: Patient-derived olfactory stem cells: New models for brain diseases. *Stem Cells* 30:2361–2365.
 28. Fan Y, Abrahamsen G, McGrath JJ, Mackay-Sim A (2012): Altered cell cycle dynamics in schizophrenia. *Biol Psychiatry* 71:129–135.
 29. Zaidel-Bar R, Itzkovitz S, Ma'ayan A, Iyengar R, Geiger B (2007): Functional atlas of the integrin adhesome. *Nat Cell Biol* 9:858–867.
 30. Dubash AD, Menold MM, Samson T, Boulter E, Garcia-Mata R, Doughman R, *et al.* (2009): Focal adhesions: New angles on an old structure. *Int Rev Cell Mol Biol* 277:1–65.
 31. Romer LH, Birukov KG, Garcia JG (2006): Focal adhesions: Paradigm for a signaling nexus. *Circ Res* 98:606–616.
 32. Berrier AL, Yamada KM (2007): Cell-matrix adhesion. *J Cell Physiol* 213: 565–573.
 33. Thiery JP (2003): Cell adhesion in development: A complex signaling network. *Curr Opin Genet Dev* 13:365–371.
 34. Brennand KJ, Simone A, Jou J, Gelboin-Burkhardt C, Tran N, Sangar S, *et al.* (2011): Modelling schizophrenia using human induced pluripotent stem cells. *Nature* 473:221–225.
 35. Castle DJ, Jablensky A, McGrath JJ, Carr V, Morgan V, Waterreus A, *et al.* (2006): The diagnostic interview for psychoses (DIP): Development, reliability and applications. *Psychol Med* 36:69–80.
 36. Association AP (1994): *Diagnostic and Statistical Manual of Mental Disorders, 4th ed.* Washington, DC: American Psychiatric Association.
 37. Doran MR, Mills RJ, Parker AJ, Landman KA, Cooper-White JJ (2009): A cell migration device that maintains a defined surface with no cellular damage during wound edge generation. *Lab Chip* 9:2364–2369.
 38. Cooley MA, Broome JM, Ohngemach C, Romer LH, Schaller MD (2000): Paxillin binding is not the sole determinant of focal adhesion localization or dominant-negative activity of focal adhesion kinase/focal adhesion kinase-related nonkinase. *Mol Biol Cell* 11:3247–3263.
 39. Goetz JG, Joshi B, Lajoie P, Strugnell SS, Scudamore T, Kojic LD, *et al.* (2008): Concerted regulation of focal adhesion dynamics by galectin-3 and tyrosine-phosphorylated caveolin-1. *J Cell Biol* 180:1261–1275.
 40. Avalos AM, Arthur WT, Schneider P, Quest AF, Burrige K, Leyton L (2004): Aggregation of integrins and RhoA activation are required for Thy-1-induced morphological changes in astrocytes. *J Biol Chem* 279: 39139–39145.
 41. Davis JM (1976): Comparative doses and costs of antipsychotic medication. *Arch Gen Psychiatry* 33:858–861.
 42. Delorme B, Nivet E, Gaillard J, Hauptl T, Ringe J, Deveze A, *et al.* (2010): The human nose harbors a niche of olfactory ectomesenchymal stem cells displaying neurogenic and osteogenic properties. *Stem Cells Dev* 19:853–866.
 43. Melton AC, Soon RK Jr, Park JG, Martinez L, Dehart GW, Yee HF Jr (2007): Focal adhesion disassembly is an essential early event in hepatic stellate cell chemotaxis. *Am J Physiol Gastrointest Liver Physiol* 293:G1272–G1280.
 44. Rodriguez Fernandez JL, Geiger B, Salomon D, Ben-Ze'ev A (1993): Suppression of vinculin expression by antisense transfection confers changes in cell morphology, motility, and anchorage-dependent growth of 3T3 cells. *J Cell Biol* 122:1285–1294.
 45. Girault JA, Costa A, Derkinderen P, Studler JM, Toutant M (1999): FAK and PYK2/CAKbeta in the nervous system: A link between neuronal activity, plasticity and survival? *Trends Neurosci* 22:257–263.
 46. Nikolic M (2004): The molecular mystery of neuronal migration: FAK and Cdk5. *Trends Cell Biol* 14:1–5.
 47. Zamir E, Geiger B (2001): Molecular complexity and dynamics of cell-matrix adhesions. *J Cell Sci* 114:3583–3590.
 48. Ruest PJ, Roy S, Shi E, Mernaugh RL, Hanks SK (2000): Phosphospecific antibodies reveal focal adhesion kinase activation loop phosphorylation in nascent and mature focal adhesions and requirement for the autophosphorylation site. *Cell Growth Differ* 11:41–48.
 49. Ridley AJ, Schwartz MA, Burridge K, Firtel RA, Ginsberg MH, Borisy G, *et al.* (2003): Cell migration: Integrating signals from front to back. *Science* 302:1704–1709.
 50. Webb DJ, Donais K, Whitmore LA, Thomas SM, Turner CE, Parsons JT, *et al.* (2004): FAK-Src signalling through paxillin, ERK and MLCK regulates adhesion disassembly. *Nat Cell Biol* 6:154–161.
 51. Gallant ND, Michael KE, Garcia AJ (2005): Cell adhesion strengthening: Contributions of adhesive area, integrin binding, and focal adhesion assembly. *Mol Biol Cell* 16:4329–4340.
 52. Xu Y, Benlimame N, Su J, He Q, Alaoui-Jamali MA (2009): Regulation of focal adhesion turnover by ErbB signalling in invasive breast cancer cells. *Br J Cancer* 100:633–643.
 53. Humphries JD, Byron A, Humphries MJ (2006): Integrin ligands at a glance. *J Cell Sci* 119:3901–3903.
 54. Fatemi SH (2001): Reelin mutations in mouse and man: From reeler mouse to schizophrenia, mood disorders, autism and lissencephaly. *Mol Psychiatry* 6:129–133.
 55. Millar JK, Christie S, Anderson S, Lawson D, Hsiao-Wei Loh D, Devon RS, *et al.* (2001): Genomic structure and localisation within a linkage hotspot of Disrupted In Schizophrenia 1, a gene disrupted by a translocation segregating with schizophrenia. *Mol Psychiatry* 6: 173–178.
 56. Stefansson H, Sarginson J, Kong A, Yates P, Steinthorsdottir V, Gudfinnsson E, *et al.* (2003): Association of neuregulin 1 with schizophrenia confirmed in a Scottish population. *Am J Hum Genet* 72: 83–87.
 57. Lee FH, Fadel MP, Preston-Maher K, Cordes SP, Clapcote SJ, Price DJ, *et al.* (2011): Disc1 point mutations in mice affect development of the cerebral cortex. *J Neurosci* 31:3197–3206.
 58. Anton ES, Kreidberg JA, Rakic P (1999): Distinct functions of alpha3 and alpha(v) integrin receptors in neuronal migration and laminar organization of the cerebral cortex. *Neuron* 22:277–289.
 59. Beggs HE, Schahin-Reed D, Zang K, Goebels S, Nave KA, Gorski J, *et al.* (2003): FAK deficiency in cells contributing to the basal lamina results in cortical abnormalities resembling congenital muscular dystrophies. *Neuron* 40:501–514.
 60. Mei L, Xiong WC (2008): Neuregulin 1 in neural development, synaptic plasticity and schizophrenia. *Nat Rev Neurosci* 9:437–452.
 61. Frotscher M (2010): Role for Reelin in stabilizing cortical architecture. *Trends Neurosci* 33:407–414.
 62. Burgaya F, Menegon A, Menegoz M, Valtorta F, Girault JA (1995): Focal adhesion kinase in rat central nervous system. *Eur J Neurosci* 7: 1810–1821.
 63. Beauvais-Jouneau A, Thiery JP (1997): Multiple roles for integrins during development. *Biol Cell* 89:5–11.
 64. Tsuji T (2004): Physiological and pathological roles of alpha3beta1 integrin. *J Membr Biol* 200:115–132.
 65. Cox BD, Natarajan M, Stettner MR, Gladson CL (2006): New concepts regarding focal adhesion kinase promotion of cell migration and proliferation. *J Cell Biochem* 99:35–52.
 66. Hill MJ, Jeffries AR, Dobson RJ, Price J, Bray NJ (2012): Knockdown of the psychosis susceptibility gene ZNF804A alters expression of genes involved in cell adhesion. *Hum Mol Genet* 21:1018–1024.